

Restricted Enumerations by the Unit-Subduced-Cycle-Index (USCI) Approach. II. Restricted Subduced Cycle Indices for Treating Interactions Between Two or More Orbits

Shinsaku Fujita

Shonan Institute of Chemoinformatics and Mathematical Chemistry,
Kaneko 479-7 Ooimachi, Ashigara-Kami-Gun, Kanagawa-Ken,
258-0019 Japan

E-mail: shinsaku_fujita@nifty.com

(Received September 1, 2011)

Abstract

The restricted-fixed-point-matrix (RFPM) method is developed as an extension of the fixed-point-matrix (FPM) method, which is one of the four methods of the unit-subduced-cycle-index (USCI) approach (S. Fujita, "Symmetry and Combinatorial Enumeration in Chemistry", Springer-Verlag (1991)). The RFPM method is capable of combinatorial enumerations of 3D structures or graphs under a restricted condition, where orbits of vertices and edges interact each other. Subduced cycle indices with chirality fittingness (SCI-CFs), which are calculated for an unrestricted condition by starting from unit subduced cycle indices with chirality fittingness (USCI-CFs), are converted into restricted SCI-CFs by means of newly-defined territory indicators (TIs) of vertices and edges. Such restricted SCI-CFs as calculated for respective subgroups are effective to evaluate the numbers of fixed points (promolecules) on the action of the subgroups under the restricted condition, where the occupation of a common vertex or the occupation of adjacent edges is avoided.

1 Introduction

Among the four methods supported by the unit-subduced-cycle-index (USCI) approach [1, 2], the fixed-point matrix (FPM) method [3–5] is based on generating functions derived from sub-

duced cycle indices (SCIs) and mark tables, where each subduced cycle index (SCI) is defined as a product of unit subduced cycle indices (USCIs). These USCIs (without chirality fittingness), or unit subduced cycle indices with chirality fittingness (USCI-CFs) as more sophisticated forms, are beforehand calculated on the basis of the concepts of *subduction of coset representations* and *sphericities*.

The FPM method has been applied to enumerations of various types, where vertices of a given skeleton (a graph or a three-dimensional structure) are considered to be main sites of substitutions [3, 6, 7]. Edges of a given skeleton have also been considered to be substitution sites [8–13]. In these enumerations, equivalent classes (orbits) of vertices or edges as substitution sites are presupposed to exhibit independent behaviors. This means the presupposition of an unrestricted condition in which substituents are considered to be able to occupy a common vertex (by a monodentate ligand and a bidentate ligand) or adjacent edges (by bidentate ligands) freely. However, the occupation of a common vertex or adjacent edges should be carefully examined according to models adopted for enumerations. For example, the occupation of adjacent edges is theoretically permissible in the numeration of organic reactions by counting substructures of imaginary transition structures [11, 14]. On the other hand, the occupation of adjacent edges occurs in counting edge configurations on a regular octahedron under the unrestricted condition [13], where the occupied adjacent edges are tentatively interpreted to be tridentate or higher ligands of various types in place of bidentate ligands. Rigorously speaking, however, the occupation of adjacent edges by bidentate ligands are not permitted.

The next task is to extend the USCI approach, which becomes capable of restricted enumerations, where orbits of vertices and edges would interact each other so as to exhibit dependent behaviors [15]. Hence, the purpose of the present article is to develop such an extended version of the USCI approach, which allows us to enumerate restricted cases of chemical compounds as three-dimensional (3D) structures as well as graphs. In particular, the FPM method is extended to develop the restricted FPM (RFPM) method, which is applicable to such restricted cases by calculating restricted SCI-CFs, where the concepts of proligands and promolecules are coupled with the concept of *chirality fittingness*.

2 Preliminaries. Unrestricted Enumerations

Before we start the formulation of restricted enumerations, we begin with SCI-CFs for unrestricted enumerations. The (unrestricted) SCI-CFs will be converted into restricted SCI-CFs in the next section, so as to formulate restricted enumerations.

2.1 SCI-CFs for Unrestricted Enumerations

In the USCI approach [1], the substitution sites (vertices, edges, etc.) of a given skeleton are divided into equivalence classes (orbits). The scheme and the symbols represented by Fig. 9.1 of [1] are adopted here. Thus, let us consider a given skeleton of a point group \mathbf{G} containing an assembly of such orbits, which are denoted by the symbol $\Delta_{i\alpha}$, where the every orbits, each governed by a coset representation $\mathbf{G}/(\mathbf{G}_i)$, are differentiated from each other by an added symbol α ($\alpha = 1, 2, \dots, \alpha_i$ if $\alpha_i \neq 0$). When there are no orbits of $\mathbf{G}/(\mathbf{G}_i)$, we place $\alpha_i = 0$. When the skeleton is fixed by a subgroup \mathbf{G}_j , each orbit $\Delta_{i\alpha}$ is subdivided in accord with the subduction of the coset representation denoted by $\mathbf{G}/(\mathbf{G}_i) \downarrow \mathbf{G}_j$ so as to generate a set of suborbits $\Delta_{jk\beta}^{(i\alpha)}$, which are differentiated from each other by an added symbol β and the coset

representation $\mathbf{G}_j(//\mathbf{G}_k^{(j)})$ assigned to each suborbit. The resulting suborbit is characterized by a sphericity index (SI) collectively represented by the symbol $\$_{d_{jk}}^{(i\alpha)}$, which is assigned to the coset representation $\mathbf{G}_j(//\mathbf{G}_k^{(j)})$, where the symbol $\$_{d_{jk}}^{(i\alpha)}$ represents an SI $a_{d_{jk}}^{(i\alpha)}$ for a homospheric orbit (\mathbf{G}_j : achiral; and $\mathbf{G}_k^{(j)}$: achiral), an SI $b_{d_{jk}}^{(i\alpha)}$ for a hemispheric orbit (\mathbf{G}_j : chiral; and $\mathbf{G}_k^{(j)}$: chiral), and an SI $c_{d_{jk}}^{(i\alpha)}$ for an enantiospheric orbit (\mathbf{G}_j : achiral; and $\mathbf{G}_k^{(j)}$: chiral), as well as we place $d_{jk} = |\mathbf{G}_j|/|\mathbf{G}_k^{(j)}|$. Note that the same $\$_{d_{jk}}^{(i\alpha)}$ is assigned to the suborbits $\Delta_{jk\beta}^{(i\alpha)}$ although these orbits are differentiated by means of β so long as they are contained in the orbit $\Delta_{i\alpha}$.

In accord with Eq. 19.4 due to Def. 9.3 of [1], a unit subduced cycle index with chirality fittingness (USCI-CF), which is represented by the symbol $\text{ZC}(\mathbf{G}/(\mathbf{G}_i) \downarrow \mathbf{G}_j; \$_{d_{jk}}^{(i\alpha)})$, is defined as a product of such sphericity indices (SIs) of the suborbits $\Delta_{jk\beta}^{(i\alpha)}$ which are contained in the orbit $\Delta_{i\alpha}$. The USCI approach precedently calculates USCI-CFs and the corresponding degenerate monomials (unit subduced cycle indices without chirality fittingness, USCIs), which are collected in a tabular form to generate a USCI-CF table for each point group, e.g., Appendices D and E of [1].

To evaluate the number of fixed derivatives under the action of a subgroup \mathbf{G}_j ($\mathbf{G}_j \subset \mathbf{G}$) by starting from the skeleton of \mathbf{G} -symmetry, a product of USCI-CFs for each subgroup \mathbf{G}_j is calculated with respect to the above-mentioned assembly of orbits ($\Delta_{i\alpha}$) according to Def. 19.3 of Ref. [1], so as to generate the corresponding SCI-CF for the assembly of orbits at issue:

$$\text{SCI-CF}(\mathbf{G}_j; \$_{d_{jk}}^{(i\alpha)}) = \prod_{i=1}^s \prod_{\substack{\alpha=1 \\ \alpha_i \neq 0}}^{\alpha_i} \text{ZC}(\mathbf{G}/(\mathbf{G}_i) \downarrow \mathbf{G}_j; \$_{d_{jk}}^{(i\alpha)}). \quad (1)$$

Such an SCI-CF as shown in Eq. 1 is capable of evaluating the number of fixed promolecules, where an appropriate set of inventory functions (cf. Lemma 19.2 of [1]) is introduced into the right-hand side of Eq. 1 to give generating functions for the subgroups \mathbf{G}_j . Because the formulation of obtaining such generating functions has been already described in Chapter 19 of [1], it is not repeated here, but its applications are illustrated by examples suitable for the purpose of this article.

2.2 Problem Setting Due to Unrestricted Enumerations

Let us consider a trigonal prismatic skeleton (**1**), which, for example, appears in the trigonal prismatic structure of *trans*-1,2-diphenylethene-1,2-dithiolato)rhenium ($[\text{Re}(\text{S}_2\text{C}_2\text{Ph}_2)_3]$) as cited in a textbook [16, page 1074]. To treat such rhenium complexes as a target of combinatorial enumeration, edge substitutions by bidentate ligands should be taken into consideration in addition to vertex substitutions by monodentate ligands. Thus the rhenium complex $[\text{Re}(\text{S}_2\text{C}_2\text{Ph}_2)_3]$ is schematically represented by the formula **2**, where the three edges $\{1,4\}$, $\{2,5\}$, and $\{3,6\}$ are occupied by three bidentate ligands (boldfaced straight lines).

Let us consider the six vertices of **1** (for monodentate ligands) and the nine edges (for bidentate ligands) as substitution sites for combinatorial enumeration. The six vertices of **1** are equivalent to construct a six-membered orbit $\{1,2,3,4,5,6\}$ governed by the coset representation $\mathbf{D}_{3h}/(\mathbf{C}_s)$. Among the nine edges, the six edges contained in the top and the bottom face are equivalent to construct a six-membered orbit $\{\{1,2\}, \{2,3\}, \{3,1\}, \{4,5\}, \{5,6\}, \{6,4\}\}$,

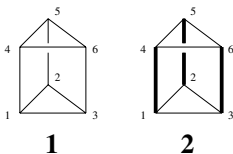


Figure 1: Trigonal prismatic skeleton and an example of its edge substitution

Table 1: SCI-CFs and Restricted SCI-CFs for a trigonal prismatic skeleton

subgroup	(Unrestricted) SCI-CF			Restricted SCI-CF
\mathbf{G}_j	Vertices	\times Edges	\times Edges	(SCI-CF)
\mathbf{C}_1	b_1^6	\tilde{b}_1^6	\hat{b}_1^3	$b_1^6 + 6b_1^2\tilde{b}_1\hat{b}_1 + 3b_1^2\hat{b}_1^2 + 9b_1^2\tilde{b}_1^2 + 3b_1^4\hat{b}_1 + 6b_1^4\tilde{b}_1 + 3\tilde{b}_1^2\hat{b}_1 + \hat{b}_1^3$
\mathbf{C}_2	b_2^3	\tilde{b}_2^3	$\hat{b}_1\hat{b}_2$	$b_2^3 + b_2^2\hat{b}_1 + 3b_2\tilde{b}_2 + b_2\hat{b}_2 + \tilde{b}_2\hat{b}_1 + \hat{b}_1\hat{b}_2$
\mathbf{C}_s	$a_1^2c_2^2$	$\tilde{a}_1^2\tilde{c}_2^2$	$\hat{a}_1\hat{c}_2$	$a_1^2c_2^2 + 2c_2\tilde{a}_1\hat{a}_1 + 2a_1^2c_2\tilde{a}_1 + a_1^2\tilde{a}_1^2 + c_2^2\hat{a}_1 + \tilde{a}_1^2\hat{a}_1 + a_1^2\tilde{c}_2 + \tilde{a}_1\hat{c}_2$
\mathbf{C}'_s	c_2^3	\tilde{c}_2^3	\hat{a}_1^3	$c_2^3 + \hat{a}_1^3 + 3\tilde{c}_2\hat{a}_1 + 3c_2\tilde{c}_2 + 3c_2^2\hat{a}_1 + 3c_2\hat{a}_1^2$
\mathbf{C}_3	b_3^3	\tilde{b}_3^3	\hat{b}_3	$b_3^3 + \hat{b}_3$
\mathbf{C}_{2v}	a_2c_4	$\tilde{a}_2\tilde{c}_4$	$\hat{a}_1\hat{a}_2$	$a_2c_4 + a_2\tilde{a}_2 + a_2\hat{a}_2 + \hat{a}_1\hat{a}_2 + \tilde{a}_2\hat{a}_1 + c_4\hat{a}_1$
\mathbf{C}_{3v}	a_3^2	\tilde{a}_3^2	\hat{a}_3	$a_3^2 + \hat{a}_3$
\mathbf{C}_{3h}	c_6	\tilde{c}_6	\hat{a}_3	$c_6 + \hat{a}_3$
\mathbf{D}_3	b_6	\tilde{b}_6	\hat{b}_3	$b_6 + \hat{b}_3$
\mathbf{D}_{3h}	a_6	\tilde{a}_6	\hat{a}_3	$a_6 + \hat{a}_3$

which is governed by the coset representation $\mathbf{D}_{3h}/(\mathbf{C}_s)$. The remaining three edges are equivalent to construct a three-membered orbit $\{\{1, 4\}, \{2, 5\}, \{3, 6\}\}$, which is governed by the coset representation $\mathbf{D}_{3h}/(\mathbf{C}_{2v})$.

The USCI-CFs for \mathbf{D}_{3h} have been already precalculated and reported in Table E.13 of [1]. Related enumerations based on several \mathbf{D}_{3h} -skeletons (a trigonal bipyramid, an iceane skeleton, and a prismane skeleton) have been reported as well as the data of the point group \mathbf{D}_{3h} [10]. From the USCI-CF table [1, 10], the $\mathbf{D}_{3h}/(\mathbf{C}_s)$ -row for the vertices and the six edges and the $\mathbf{D}_{3h}/(\mathbf{C}_{2v})$ -row for the three edges are cited and listed in the Vertices-column (USCI-CF as a product of SIs without accents), the Edges-column (USCI-CF as a product of SIs with tilde accents), and the other Edges-column (USCI-CF as a product of SIs with hat accents) of Table 1. The three types of USCI-CFs for each subgroup are multiplied to give the corresponding (unrestricted) SCI-CF. Note that the superscript $(i\alpha)$ of $S_{d_{jk}}^{(i\alpha)}$ in Eq. 1 is replaced by accent symbols for the simplicity's sake.

Suppose that monodentate ligands for vertex substitution are selected from the following inventory:

$$\mathbf{L} = \{X, p, \bar{p}\}, \quad (2)$$

which corresponds to inventory functions:

$$a_d = 1 + X^d \quad (3)$$

$$b_d = 1 + X^d + p^d + \bar{p}^d \quad (4)$$

$$c_d = 1 + X^d + 2p^{d/2}\bar{p}^{d/2} \quad (5)$$

where X represents an achiral monodentate ligand and p/\bar{p} represents a pair of enantiomeric monodentate ligands in isolation. It should be noted that the power $d/2$ appearing in Eq. 5 is an integer because the subscript d of c_d is always even in the light of the enantiosphericity of the corresponding orbit. The term 1 in the right-hand sides of Eqs. 3–5 represents an implicit substituent (H or no substitution).

And suppose that bidentate ligands for edge substitution are selected following inventory:

$$L' = \{Z\}, \quad (6)$$

which corresponds to inventory functions:

$$\tilde{a}_d = \tilde{b}_d = \tilde{c}_d = 1 + Z^d \quad (7)$$

$$\hat{a}_d = \hat{b}_d = \hat{c}_d = 1 + Z^d \quad (8)$$

where we here only one type of bidentate ligands (Z) with no chirality and no direction. The term 1 in the right-hand sides represents no substitution on edges.

These inventory functions for vertices (Eqs. 3–5) and for edges (Eqs. 7 and 8) are introduced into an SCI-CF to give a generating function, in which the coefficient of the term $X^k p^\ell \bar{p}^m Z^n$ indicates the number of fixed promolecules to be counted. The term can be represented by the following partition:

$$[\theta] = [k; \ell, m; n]. \quad (9)$$

For example, let us examine the SCI-CF for the subgroup C_s , i.e., $(a_1^2 c_2^2)(\tilde{a}_1^2 \tilde{c}_2^2)(\hat{a}_1 \hat{c}_2)$, among the SCI-CFs of **1** listed in Table 1. The inventory functions for vertices (Eqs. 3–5) and for edges (Eqs. 7 and 8) are introduced into this SCI-CF and the resulting equation is expanded to give the following generating function:

$$\begin{aligned} g_{C_s} = & 1 + 4p\bar{p} + 2X + 8X^2 p\bar{p} + 4p^2 \bar{p}^2 + 4X^3 + 8Xp\bar{p} + 2X^5 + 8X^3 p\bar{p} + \dots \\ & + (3 + 6X + 12p^2 \bar{p}^2 + 24Xp\bar{p} + 12p\bar{p} + 9X^4 + 24X^2 p\bar{p} + 9X^2 + 12X^3 + \dots)Z \\ & + (6 + 12X + 48Xp^2 \bar{p}^2 + 48Xp\bar{p} + 24X^2 p^2 \bar{p}^2 + 24X^3 + 18X^2 + 24p\bar{p} + \dots)Z^2 \\ & + (10 + 20X + 30X^2 + 40p^2 \bar{p}^2 + 80X^2 p\bar{p} + 80X^3 p\bar{p} + \dots)Z^3 + \dots \end{aligned} \quad (10)$$

According to Lemma 19.2 of [1], the coefficient of each term appearing in the right-hand side of Eq. 10, which is denoted by the symbol $\rho_{[\theta]C_s}$ ($\rho_{[\theta]G_j}$ in general), represents the number of fixed promolecules of C_s (G_j in general), where the symbol $[\theta]$ is shown in Eq. 9. Among them, we here focus on the term Z^3 , which corresponds to the partition:

$$[\theta]_1 = [0; 0, 0; 3]. \quad (11)$$

Thereby, the coefficient 10 of $10Z^3$ in the right-hand side of Eq. 10 indicates the number ($\rho_{[\theta]_1 C_s}$) of fixed promolecules of the term Z^3 or the partition $[\theta]_1$ under the action of the subgroup C_s , i.e.,

$$\rho_{[\theta]_1 C_s} = 10. \quad (12)$$

This process for obtaining $\rho_{[\theta]_1\mathbf{C}_s}$ is repeated to cover all of the subgroup \mathbf{G}_j to give $\rho_{[\theta]_1\mathbf{G}_j}$ ($\mathbf{G}_j \subset \mathbf{D}_{3h}$), which are collected to form a fixed-point vector (FPV) as follows:

$$\text{FPV}_1 = (\rho_{[\theta]_1\mathbf{C}_1}, \rho_{[\theta]_1\mathbf{C}_2}, \rho_{[\theta]_1\mathbf{C}_s}, \dots, \rho_{[\theta]_1\mathbf{D}_{3h}}) = (84, 4, 10, 10, 3, 2, 3, 1, 1, 1). \quad (13)$$

Note that the elements in Eq. 13 are aligned in accord with the appearance order of the respective subgroups shown in the first column of Table 1, which are collectively called by a name “the non-redundant set of subgroups of \mathbf{D}_{3h} ” and denoted by the symbol $\text{SSG}_{\mathbf{D}_{3h}}$. FPVs for other partitions, e.g.,

$$[\theta]_2 = [0; 0, 0; 0] \quad (\text{for } 1) \quad (14)$$

$$[\theta]_3 = [0; 0, 0; 1] \quad (\text{for } Z) \quad (15)$$

$$[\theta]_4 = [0; 0, 0; 2] \quad (\text{for } Z^2) \quad (16)$$

$$[\theta]_5 = [0; 1, 1; 0] \quad (\text{for } p\bar{p}) \quad (17)$$

$$[\theta]_6 = [1; 1, 1; 0] \quad (\text{for } Xp\bar{p}) \quad (18)$$

$$[\theta]_7 = [0; 1, 1; 1] \quad (\text{for } p\bar{p}Z) \quad (19)$$

$$[\theta]_8 = [1; 1, 1; 1] \quad (\text{for } Xp\bar{p}Z), \quad (20)$$

are similarly obtained and collected to form a fixed-point matrix (FPM), in which each FPV is contained as a row vector as follows:

$$\text{FPM}_1 = \begin{matrix} [\theta]_2 \\ [\theta]_3 \\ [\theta]_4 \\ [\theta]_1 \\ [\theta]_5 \\ [\theta]_6 \\ [\theta]_7 \\ [\theta]_8 \end{matrix} \begin{pmatrix} 1 & 1 & 1 & 1 & 1 & 1 & 1 & 1 & 1 & 1 \\ 9 & 1 & 3 & 3 & 0 & 1 & 0 & 0 & 0 & 0 \\ 36 & 4 & 6 & 6 & 0 & 2 & 0 & 0 & 0 & 0 \\ 84 & 4 & 10 & 10 & 3 & 2 & 3 & 1 & 1 & 1 \\ 30 & 0 & 4 & 6 & 0 & 0 & 0 & 0 & 0 & 0 \\ 120 & 0 & 8 & 0 & 0 & 0 & 0 & 0 & 0 & 0 \\ 270 & 0 & 12 & 18 & 0 & 0 & 0 & 0 & 0 & 0 \\ 1080 & 0 & 24 & 0 & 0 & 0 & 0 & 0 & 0 & 0 \end{pmatrix}. \quad (21)$$

Note the FPV_1 for the partition $[\theta]_1$ (Eq. 13) appears at the 4th row of the FPM_1 (Eq. 21). The values appearing at the third column (the \mathbf{C}_s -column) of FPM_1 (Eq. 21) are collected from the generating function for \mathbf{C}_s (Eq. 10), e.g., the term $3Z$ of Eq. 10 corresponds to the value 3 at the intersection of the $[\theta]_3$ -row and the \mathbf{C}_s -column.

Because the FPM (Eq. 21) contains FPVs as its row vectors, Theorem 19.2 (or Theorem 15.4) can be applied. Thus, the FPM is multiplied by the inverse mark table $M_{\mathbf{D}_{3h}}^{-1}$ (Table B.13 of [1]) so as to give an isomer-counting matrix (ICM):

$$\text{ICM}_1 = \text{FPM}_1 \times M_{\mathbf{D}_{3h}}^{-1} \\ = \text{FPM}_1 \times \begin{pmatrix} \frac{1}{12} & 0 & 0 & 0 & 0 & 0 & 0 & 0 & 0 & 0 \\ -\frac{1}{4} & \frac{1}{2} & 0 & 0 & 0 & 0 & 0 & 0 & 0 & 0 \\ -\frac{1}{4} & 0 & \frac{1}{2} & 0 & 0 & 0 & 0 & 0 & 0 & 0 \\ -\frac{1}{12} & 0 & 0 & \frac{1}{6} & 0 & 0 & 0 & 0 & 0 & 0 \\ -\frac{1}{12} & 0 & 0 & 0 & \frac{1}{4} & 0 & 0 & 0 & 0 & 0 \\ \frac{1}{2} & -\frac{1}{2} & -\frac{1}{2} & -\frac{1}{2} & 0 & 1 & 0 & 0 & 0 & 0 \\ \frac{1}{4} & 0 & -\frac{1}{2} & 0 & -\frac{1}{4} & 0 & \frac{1}{2} & 0 & 0 & 0 \\ \frac{1}{12} & 0 & 0 & -\frac{1}{6} & -\frac{1}{4} & 0 & 0 & \frac{1}{2} & 0 & 0 \\ \frac{1}{4} & 0 & -\frac{1}{2} & 0 & -\frac{1}{4} & 0 & 0 & 0 & \frac{1}{2} & 0 \\ -\frac{1}{2} & \frac{1}{2} & \frac{1}{2} & \frac{1}{2} & \frac{1}{2} & -1 & -\frac{1}{2} & -\frac{1}{2} & -\frac{1}{2} & 1 \end{pmatrix} = \begin{matrix} [\theta]_2 \\ [\theta]_3 \\ [\theta]_4 \\ [\theta]_1 \\ [\theta]_5 \\ [\theta]_6 \\ [\theta]_7 \\ [\theta]_8 \end{matrix} \begin{pmatrix} 0 & 0 & 0 & 0 & 0 & 0 & 0 & 0 & 0 & 1 \\ 0 & 0 & 1 & 0 & 0 & 1 & 0 & 0 & 0 & 0 \\ 1 & 1 & 2 & 0 & 0 & 2 & 0 & 0 & 0 & 0 \\ 4 & 1 & 3 & 1 & 0 & 1 & 1 & 0 & 0 & 1 \\ 1 & 0 & 2 & 1 & 0 & 0 & 0 & 0 & 0 & 0 \\ 8 & 0 & 4 & 0 & 0 & 0 & 0 & 0 & 0 & 0 \\ 18 & 0 & 6 & 3 & 0 & 0 & 0 & 0 & 0 & 0 \\ 84 & 0 & 12 & 0 & 0 & 0 & 0 & 0 & 0 & 0 \end{pmatrix}, \quad (22)$$

where each pair of enantiomers is counted once just as each achiral derivative is counted once. As a matter of course, additional rows of other partitions can be freely inserted to such an FPM as Eq. 21 in accord with targets of enumerations.

As an exemplified verification of the results shown in the ICM₁ (Eq. 22), let us examine the $[\theta]_1$ -row, which indicates the presence of four enantiomeric pairs of \mathbf{C}_1 -derivatives (**3** $\bar{3}$, **4** $\bar{4}$, **5** $\bar{5}$, and **6** $\bar{6}$), one enantiomeric pair of \mathbf{C}_2 -derivatives (**7** $\bar{7}$), three \mathbf{C}_s -derivatives (**8**, **9**, and **10**), one \mathbf{C}'_s -derivative (**11**), one \mathbf{C}_{2v} -derivative (**12**), one \mathbf{C}_{3v} -derivative (**13**), and one \mathbf{D}_{3h} -derivative (**14**). These derivatives are illustrated in Fig. 2.

It should be noted that the derivatives shown in Fig. 2 (except **12** (\mathbf{C}_{2v}) and **14** ($= \mathbf{2}, \mathbf{D}_{3h}$)) have one or more vertices which accommodate two or more terminals of bidentate ligands. Chemically speaking, these derivatives may be interpreted as accommodating tridentate or higher ligands of various types. When substituents are restricted to monodentate or bidentate ligands, however, only **12** (\mathbf{C}_{2v}) and **14** ($= \mathbf{2}, \mathbf{D}_{3h}$) should be adopted to treat resulting metal complexes properly. This type of restricted enumeration is the target of the following part of the present article.

3 Restricted Enumeration

3.1 Territory Indicators

To take a hint to conduct such restricted enumeration, let us examine the derivatives of Z^3 ($[\theta]_1$) shown in Fig. 2 in detail. The \mathbf{C}_1 -derivative **3** has edge substitutions at the edges $\{1, 2\}$, $\{4, 6\}$, and $\{2, 5\}$, where the edges $\{1, 2\}$ and $\{2, 5\}$ have a common vertex $\{2\}$. Dummy variables x_1x_2 , x_4x_6 , and x_2x_5 are assigned to the respective edges, where the subscripts represent their terminal vertices. Because the product of them, i.e., $(x_1x_2)(x_4x_6)(x_2x_5) = x_1x_2^2x_4x_5x_6$, characterizes the mode of edge substitution, it is called a *territory indicator* (TI). Thus, the second power of x_2 of the TI indicates the overlap of two edge substituents at the vertex $\{2\}$, which is determined to suffer from multiple occupation. The TIs of the derivatives shown in Fig. 2 are collected also in Fig. 2. By examining them, the derivatives except **12** (\mathbf{C}_{2v}) and **14** ($= \mathbf{2}, \mathbf{D}_{3h}$) are characterized by territory indicators having the second power of at least one dummy variable. On the other hand, **12** (\mathbf{C}_{2v}) and **14** ($= \mathbf{2}, \mathbf{D}_{3h}$) have a TI, $x_1x_2x_3x_4x_5x_6$, in which each dummy variable x_i appears only once so as to assure the absence of vertices of multiple occupation.

The \mathbf{C}_{2v} -derivative **12** is characterized by the SCI-CF $(a_2c_4)(\tilde{a}_2\tilde{c}_4)(\hat{a}_1\hat{a}_2)$ in the \mathbf{C}_{2v} -row of Table 1, where a one-membered orbit of one edge $\{1, 4\}$ is ascribed to the SI \hat{a}_1 , while a two-membered orbit of two edges $\{2, 3\}$, $\{5, 6\}$ is ascribed to the SI \tilde{a}_2 . Hence, we are able to define combined monomials, $\hat{a}_1x_1x_4$ and $\tilde{a}_2x_2x_3x_5x_6$, where the part x_1x_4 or $x_2x_3x_5x_6$ is here called a *territory indicator for the orbit* at issue. The remaining orbits concerned with the SCI-CF are not used to generate the \mathbf{C}_{2v} -derivative **12**, so that we place $a_2 = 1$, $c_4 = 1$, $\tilde{c}_4 = 1$, and $\hat{a}_2 = 1$. Thereby, the SCI-CF $(a_2c_4)(\tilde{a}_2\tilde{c}_4)(\hat{a}_1\hat{a}_2)$ is restricted to a restricted SCI-CF $\hat{a}_1\tilde{a}_2$ via $\hat{a}_1x_1x_4 \times \tilde{a}_2x_2x_3x_5x_6 = \hat{a}_1\tilde{a}_2x_1x_2x_3x_4x_5x_6$, the TI part of which has already appeared below the formula **12** in Fig. 2 and afterward omitted for the purpose of generating the restricted SCI-CF $\hat{a}_1\tilde{a}_2$.

In a similar way, the \mathbf{D}_{3h} -derivative **14** is characterized by the SCI-CF $(a_6)(\tilde{a}_6)(\hat{a}_3)$ in the \mathbf{D}_{3h} -row of Table 1, where a three-membered orbit of edges $\{1, 4\}$, $\{2, 5\}$, $\{3, 6\}$ is ascribed to

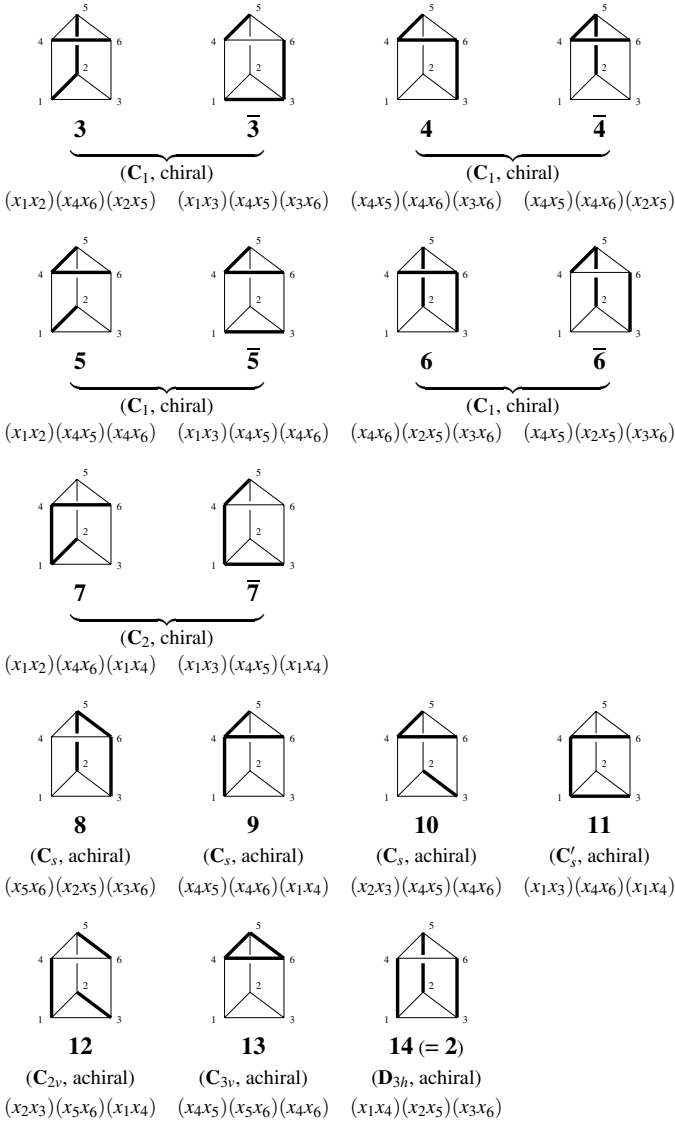


Figure 2: Derivatives of $Z^3([\theta]_1)$ by unrestricted edge substitutions and their territory indicators

the SI \hat{a}_3 . Hence, we are able to defined a combined monomial, $\hat{a}_3x_1x_4x_2x_5x_3x_6$. The remaining orbits concerned with the SCI-CF are not used to generate the \mathbf{D}_{3h} -derivative **14**, so that we place $a_6 = 1$ and $\bar{a}_6 = 1$. Thereby, the SCI-CF $(a_6)(\bar{a}_6)(\hat{a}_3)$ is converted into a restricted SCI-CF \hat{a}_3 via $\hat{a}_3x_1x_4x_2x_5x_3x_6$, the TI part of which has already appeared below the formula **14** in Fig. 2 and afterward omitted for the purpose of generating the restricted SCI-CF \hat{a}_3 .

3.2 Discriminants of SCI-CFs and Restricted SCI-CFs

The discussions in the preceding paragraphs are generalized after a dummy variable for showing the territory of an object (vertex, edge, etc.) contained in a given suborbit $\Delta_{jk\beta}^{(i\alpha)}$ is defined as x_i for a vertex $\{i\}$, $x_i x_j$ for an edge $\{i, j\}$, and so on. A territory indicator for the suborbit is defined as a product of such dummy variables as follows:

$$t_{jk}^{(i\alpha)}(x_1, \dots, x_v), \tag{23}$$

which consists of x_1, x_2, \dots, x_v in accord with the objects of the suborbit $\Delta_{jk\beta}^{(i\alpha)}$. Then, we assign $\$_{d_{jk}}^{(i\alpha)} t_{jk}^{(i\alpha)}(x_1, \dots, x_v)$ to the suborbit $\Delta_{jk\beta}^{(i\alpha)}$. For judging whether or not the suborbit is used for enumeration, the term $1 + \$_{d_{jk}}^{(i\alpha)} t_{jk}^{(i\alpha)}(x_1, \dots, x_v)$ is introduced into the original $\$_{d_{jk}}^{(i\alpha)}$ of the SCI-CF (Eq. 1) so as to give a discriminant of SCI-CF denoted by the symbol DSCI-CF.

Definition 1 The discriminant of the SCI-CF (Eq. 1) is defined as follows:

$$\text{DSCI-CF}(\mathbf{G}_j; \$_{d_{jk}}^{(i\alpha)}, x_1, x_2, \dots, x_v) = \prod_{i=1}^s \prod_{\substack{\alpha=1 \\ \alpha_i \neq 0}}^{\alpha_i} \text{ZC}(\mathbf{G}/\mathbf{G}_i) \downarrow \mathbf{G}_j; \$_{d_{jk}}^{(i\alpha)} \left| \right. \$_{d_{jk}}^{(i\alpha)} = 1 + \$_{d_{jk}}^{(i\alpha)} t_{jk}^{(i\alpha)}(x_1, \dots, x_v) \tag{24}$$

Note that the replacement of $\$_{d_{jk}}^{(i\alpha)}$ by $1 + \$_{d_{jk}}^{(i\alpha)} t_{jk}^{(i\alpha)}(x_1, \dots, x_v)$ means that the corresponding suborbit $\Delta_{jk\beta}^{(i\alpha)}$ is taken into no consideration (the former term 1) or into consideration (the latter term) during the process of enumeration. Hence, the expansion of the right-hand side of Eq. 24 generates a polynomial, where each component monomial indicates a product of SIs ($\$_{d_{jk}}^{(i\alpha)}$) as well as the corresponding product of territory indicators. Among such monomials, only monomials with $x_1 x_2 \cdots x_v$ (in which each x_i appears only once) are necessary to the process of enumeration. A monomial lacking any x_i should be rejected, because all of the vertices should be taken into consideration. Moreover, a monomial with the second or more power of x_i shows the duplication of the i -th vertex and should be rejected. After the selection of such necessary monomials is completed, the territory-indicator part of each monomial is omitted. The process described above can be conducted by the following lemma:

Lemma 1 (Restricted SCI-CFs) Among the monomials contained in the discriminant generated by Def. 1, monomials signified by the TI $x_1 x_2 \cdots x_v$ (in which each x_i appears only once) are selected by means of the following equation:

$$\overline{\text{SCI-CF}}(\mathbf{G}_j; \$_{d_{jk}}^{(i\alpha)}) = \frac{\partial^v}{\partial x_1 \partial x_2 \cdots \partial x_v} \text{DSCI-CF}(\mathbf{G}_j; \$_{d_{jk}}^{(i\alpha)}, x_1, x_2, \dots, x_v) \Big|_{x_1=x_2=\dots=x_v=0}, \tag{25}$$

where the TI part of each selected monomial is replaced by 1 (no appearance).

The proof is rather obvious. For example, the multiple partial differential according to Eq. 25 is applied to a resulting term of Eq. 24:

$$(\$_{d_{jk}}^{(i\alpha)} \cdots)(x_1 x_2 \cdots x_v) \quad (26)$$

so as to leave $(\$_{d_{jk}}^{(i\alpha)} \cdots)$, which remains even by putting $x_1 = x_2 = \cdots = x_v = 0$. The remaining term is adopted during the restricted enumeration. On the other hand, the multiple partial differential applied to another term:

$$(\$_{d_{jk}}^{(i\alpha)} \cdots)(x_1^2 x_2 \cdots x_v) \quad (27)$$

leaves $2(\$_{d_{jk}}^{(i\alpha)} \cdots)x_1$, which vanishes to zero by putting $x_1 = x_2 = \cdots = x_v = 0$. Thus, the term at issue is discarded during the restricted enumeration. Thereby, the duplicated consideration of the vertex 1 is avoided. The resulting polynomial (Eq. 25) is here called a *restricted SCI-CF*.

The restricted SCI-CF (Eq. 25) is used to evaluate the numbers of fixed points (marks) in place of the SCI-CF (Eq. 1). Lemma 19.2 of [1] for obtaining the number of fixed points (marks) ρ_{θ_j} is modified to meet the present case.

Lemma 2 (Marks for Restricted Enumerations) The marks $(\rho_{\theta_j}$'s) with weight W_{θ} 's are given by the following generation functions:

$$\sum_{[\theta]} \rho_{\theta_j} W_{\theta} = \overline{\text{SCI-CF}}(\mathbf{G}_j; \$_{d_{jk}}^{(i\alpha)}) \quad (28)$$

for $j = 1, 2, \dots, s$, where the variables $\$_{d_{jk}}^{(i\alpha)}$ ($\$ = a, b, c$) are substituted by

$$a_{d_{jk}}^{(i\alpha)} = \sum_{\ell=1}^{|\mathbf{X}|} w_{i\alpha}(\mathbf{X}_{\ell}^{(a)})^{d_{jk}} \quad (29)$$

$$b_{d_{jk}}^{(i\alpha)} = \sum_{\ell=1}^{|\mathbf{X}|} w_{i\alpha}(\mathbf{X}_{\ell})^{d_{jk}} \quad (30)$$

$$c_{d_{jk}}^{(i\alpha)} = \sum_{\ell=1}^{|\mathbf{X}|} w_{i\alpha}(\mathbf{X}_{\ell}^{(a)})^{d_{jk}} + 2 \sum_{\ell=1}^{|\mathbf{X}|} \left(w_{i\alpha}(\mathbf{X}_{\ell}^{(c)}) w_{i\alpha}(\overline{\mathbf{X}}_{\ell}^{(c)}) \right)^{d_{jk}/2}. \quad (31)$$

For the notations, see Lemma 19.2 of [1]. The proof is almost the same as Lemma 19.2 of [1], because the $\overline{\text{SCI-CF}}(\mathbf{G}_j; \$_{d_{jk}}^{(i\alpha)})$ (Eq. 25) is a definite restriction of the original SCI-CF($\mathbf{G}_j; \$_{d_{jk}}^{(i\alpha)}$) (Eq. 1), which has been used in Lemma 19.2 of [1]. It is to be noted that the marks (the numbers of fixed points) obtained by Lemma 2 can be regarded as the numbers of fixed (pro)molecules, chemically speaking, where the term *points* is abstractly used to denote molecules or pro-molecules (or other objects in general).

The marks calculated by Eq. 28 (Lemma 2) are applied to the equations of Theorem 19.4 of [1] so as to give the number (B_{θ_i}) of non-equivalent derivatives of symmetry \mathbf{G}_i under the restricted condition ($\mathbf{G}_i \subset \mathbf{G}$). The following theorem is described without a proof, because it can be proved on the same line as Theorem 19.4 of [1].

Theorem 1 (Numbers of Derivatives by Restricted Enumerations) The number B_{θ_i} of \mathbf{G}_i -derivatives of the formula $[\theta]$ under restricted enumerations is calculated by:

$$B_{\theta_i} = \sum_{j=1}^s \rho_{\theta_j} \bar{m}_{ji} \quad (32)$$

for $i = 1, 2, \dots, s$, where the ρ_{θ_j} values are calculated by Lemma 2 and the symbol \bar{m}_{ji} represents an element of the inverse mark table of the group \mathbf{G} .

When the formula $[\theta]$ is tentatively fixed, Eq. 32 of Theorem 1 is transformed into a vector calculation:

$$(B_{\theta_1}, B_{\theta_2}, \dots, B_{\theta_i}, \dots, B_{\theta_s}) = (\rho_{\theta_1}, \rho_{\theta_2}, \dots, \rho_{\theta_j}, \dots, \rho_{\theta_s}) M_{\mathbf{G}}^{-1} \quad (33)$$

where the symbol $M_{\mathbf{G}}^{-1}$ represents the inverse of the mark table $M_{\mathbf{G}}$ for the group \mathbf{G} , where the elements of $M_{\mathbf{G}}^{-1}$ are represented by \bar{m}_{ji} . The row vector in the left-hand side of Eq. 33 is called a *restricted isomer-counting vector* (RICV), while the row vector in the right-hand side of Eq. 33 is called a *restricted fixed-point vector* (RFPV). Then, Eq. 33 is symbolically represented as $\text{RICV} = \text{RFPV} \times M_{\mathbf{G}}^{-1}$. When various formulas for $[\theta]$ are considered, the RICV and the RFPV in Eq. 33 can be transformed into a restricted isomer-counting matrix (RICM) and a restricted fixed-point matrix (RFBPM) respectively, where each RICV and each RFPV are row vectors of the respective matrices. Then, the resulting matrix calculation is symbolically represented as $\text{RICM} = \text{RFBPM} \times M_{\mathbf{G}}^{-1}$.

The enumeration based on Theorem 1 is called the *restricted fixed-point-matrix (RFBPM) method*, because it is an extension of the FPM method. The terms FPV, FPM, ICM, etc. used in the FPM method are converted into RFPV (restricted FPV), RFBPM (restricted FPM), RICM (restricted ICM) etc. for the purpose of discriminating between the original FPV method and the expended version. It should noted, however, that these two sets of terms are regarded as being conceptually equivalent after marks (the numbers of fixed points) are evaluated by Lemma 2. Hence, we may sometimes adopt conventions that the terms FPV, FPM, ICM, etc. are used in place of RFPV (restricted FPV), RFBPM (restricted FPM) so long as such usage causes no confusion.

3.3 Illustrative Examples

3.3.1 Restricted SCI-CFs for the Trigonal Prismatic Skeleton

By starting from the trigonal prismatic skeleton **1**, let us consider a restricted enumeration, where any set of monodentate and bidentate ligands as substituents does not occupy a common vertex. Under this restriction condition, for example, only **12** (\mathbf{C}_{2v}) and **14** ($= \mathbf{2}, \mathbf{D}_{3h}$) should be adopted from the list shown in Fig. 2.

The \mathbf{C}_s -row of Table 1 shows that the unrestricted SCI-CF for the subgroup \mathbf{C}_s is calculated to be $(a_1^2 c_2^2)(\hat{a}_1^2 \hat{c}_2^2)(\hat{a}_1 \hat{c}_2)$. Each SI contained in the unrestricted SCI-CF corresponds to the suborbitals generated by the subduction of the \mathbf{D}_{3h} -skeleton (**1**) into the subgroup \mathbf{C}_s . Let us consider the mirror plane of the \mathbf{C}_s -group which contains the edge $\{1,3\}$ and bisects the edges $\{2,3\}$ and $\{5,6\}$. Then, the respective sphericity indices and the corresponding suborbitals are listed as follows:

(vertices):

$$a_1^2: \quad \text{two one-membered orbits } \{1\}, \{4\}$$

$$\begin{aligned}
 c_2^2 &: \text{two two-membered orbits } \{2,3\}, \{5,6\} \\
 (\text{edges}): & \\
 \tilde{a}_1^2 &: \text{two one-membered orbits } \{\{2,3\}\}, \{\{5,6\}\} \\
 \tilde{c}_2^2 &: \text{two two-membered orbits } \{\{1,2\}\}, \{\{1,3\}\}, \{\{4,5\}\}, \{4,6\} \\
 (\text{edges}): & \\
 \hat{a}_1 &: \text{one one-membered orbit } \{\{1,4\}\} \\
 \hat{c}_2 &: \text{one two-membered orbits } \{\{2,5\}\}, \{3,6\}
 \end{aligned}$$

Thereby, a TI can be easily assigned to each sphericity index. According to Eq. 24 of Def. 1, the corresponding discriminant is calculated as follows:

$$\begin{aligned}
 \text{DSCI-CF}(\mathbf{C}_s, \$d, \tilde{\$d}, \hat{\$d}, x_1, \dots, x_6) & \\
 &= (1 + a_1x_1)(1 + a_1x_4)(1 + c_2x_2x_3)(1 + c_2x_5x_6) \\
 &\quad \times (1 + \tilde{a}_1x_2x_3)(1 + \tilde{a}_1x_5x_6)(1 + \tilde{c}_2x_1x_2x_1x_3)(1 + \tilde{c}_2x_4x_5x_4x_6) \\
 &\quad \times (1 + \hat{a}_1x_1x_4)(1 + \hat{c}_2x_2x_5x_3x_6) \\
 &= (1 + a_1x_1)(1 + a_1x_4)(1 + c_2x_2x_3)(1 + c_2x_5x_6) \\
 &\quad \times (1 + \tilde{a}_1x_2x_3)(1 + \tilde{a}_1x_5x_6) \\
 &\quad \times (1 + \hat{a}_1x_1x_4)(1 + \hat{c}_2x_2x_5x_3x_6), \tag{34}
 \end{aligned}$$

where we place $(1 + \tilde{c}_2x_1x_2x_1x_3) = 1$ (the presence of x_1^2) and $(1 + \tilde{c}_2x_4x_5x_4x_6) = 1$ (the presence of x_4^2) because they are concerned with overlapped vertices and can be removed beforehand. The discriminant (Eq. 34) is treated according to Lemma 2 to give the following restricted SCI-CF:

$$\begin{aligned}
 \overline{\text{SCI-CF}}(\mathbf{C}_s; \$d, \tilde{\$d}, \hat{\$d}) &= \frac{\partial^6}{\partial x_1 \partial x_2 \dots \partial x_6} \text{DSCI-CF}(\mathbf{C}_s, \$d, \tilde{\$d}, \hat{\$d}, x_1, \dots, x_6) \Bigg|_{\substack{x_i=0 \\ (i=1, \dots, 6)}} \\
 &= a_1^2 c_2^2 + 2c_2 \tilde{a}_1 \hat{a}_1 + 2a_1^2 c_2 \tilde{a}_1 + a_1^2 \tilde{a}_1^2 + c_2^2 \hat{a}_1 + \tilde{a}_1^2 \hat{a}_1 + a_1^2 \hat{c}_2 + \tilde{a}_1 \hat{c}_2 \tag{35}
 \end{aligned}$$

The expansion and the subsequent partial differential is conducted by means of the following Maple program:

```

#prismCsA.mpl
DSCICFCs :=
(1+a1*x1) * (1+a1*x4) * (1+c2*x2*x3) * (1+c2*x5*x6)
* (1+A1*x2*x3) * (1+A1*x5*x6) * (1+AA1*x1*x4) * (1+CC2*x2*x5*x3*x6);

tempCsA := expand(DSCICFCs);
tempCsB := diff(tempCsA, x1, x2, x3, x4, x5, x6);

x1 :=0; x2 :=0; x3 :=0;
x4 :=0; x5 :=0; x6 :=0;

resSCICs := expand(tempCsB);

```

In this and related programs for calculating restricted SCI-CFs of respective subgroups, the symbol a_1, b_1, c_2 , etc. are replaced by $a1, b1, c2$, etc.; the symbol $\tilde{a}_1, \tilde{b}_1, \tilde{c}_2$, etc. are replaced by $A1, B1, C2$, etc.; and the symbol $\hat{a}_1, \hat{b}_1, \hat{c}_2$, etc. are replaced by $AA1, BB1, CC2$, and so on.

Lemma 2 means that the restricted SCI-CF (Eq. 35) is used to evaluate the number of fixed points (promolecules) on the action of the subgroup \mathbf{C}_s in place of the unrestricted (usual)

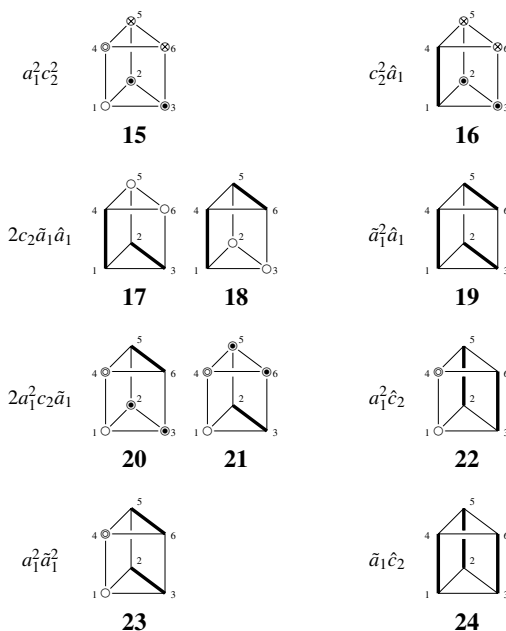


Figure 3: Possible fixed promolecules for the monomials appearing in the restricted SCI-CF (Eq. 35). These structures are fixed under the action of C_S .

SCI-CF $(a_1^2 c_2^2)(\tilde{a}_1^2 \tilde{c}_2^2)(\hat{a}_1 \hat{c}_2)$. As a result, each monomial in the restricted SCI-CF (Eq. 35) participates in the calculation of the number of fixed points (promolecules), as shown in Fig. 3, where the circles of various types denote achiral monodentate ligands, while the boldfaced straight line denotes a bidentate ligand. For example, the monomial $2c_2 \tilde{a}_1 \hat{a}_1$ appearing in Eq. 35 corresponds to **17** and **18**, where a two-membered orbit of vertices $\{5, 6\}$ (or $\{2, 3\}$) is assigned to c_2 , a one-membered orbit of an edge $\{\{2, 3\}\}$ (or $\{\{5, 6\}\}$) to \tilde{a}_1 , and a one-membered orbit of an edge $\{\{1, 4\}\}$ to \hat{a}_1 . It should be emphasized that all of the fixed promolecules shown in Fig. 3 are characterized by the absence of vertices of multiple occupation.

The process of calculating the restricted SCI-CF is repeated to cover all of the SCI-CFs listed in Table 1. The restricted SCI-CFs for every subgroups are thus calculated and collected in the rightmost column of Table 1.

While the inventory functions (Eqs. 3–5) for vertex substitution are used, the following inventory functions for edge substitutions:

$$\tilde{a}_d = \tilde{b}_d = \tilde{c}_d = Z^d \quad (36)$$

$$\hat{a}_d = \hat{b}_d = \hat{c}_d = Z^d \quad (37)$$

are used in place of Eqs. 7 and 8, because implicit edge substitutions (the term 1 deleted) are not taken into consideration. Thus, Eqs. 3–5 for vertex substitution as well as Eqs. 36 and 37

for edge substitution are introduced into Eq. 35 to give the following generating function:

$$\begin{aligned}
 g'_{C_s} = & 1 + 2X + 3X^2 + 4X^3 + 3X^4 + 2X^5 + X^6 \\
 & + 4p\bar{p} + 8Xp\bar{p} + 8X^2p\bar{p} + 8X^3p\bar{p} + 4X^4p\bar{p} + 4p^2\bar{p}^2 + 8Xp^2\bar{p}^2 + 4X^2p^2\bar{p}^2 \\
 & + (3 + 6X^2 + 8p\bar{p} + 4p^2\bar{p}^2 + 3X^4 + 8Xp\bar{p} + 8X^2p\bar{p} + 4X^3 + 4X)Z \\
 & + (4p\bar{p} + 4X + 4X^2 + 4)Z^2 + 2Z^3
 \end{aligned} \tag{38}$$

According to Lemma 2, the coefficient of each term appearing in the right-hand side of Eq. 38 represents the number of fixed promolecules of C_s , where the symbol $[\theta]$ is shown in Eq. 9. Let us consider the term Z^3 ($[\theta]_1 = [0; 0; 0; 3]$, cf. Eq. 11), the coefficient of which is equal 2, i.e.,

$$\rho_{[\theta]_1, C_s} = 2. \tag{39}$$

This process for obtaining $\rho_{[\theta]_1, C_s}$ is repeated to cover all of the subgroup G_j to give $\rho_{[\theta]_1, G_j}$ ($G_j \subset D_{3h}$), which are collected to form a restricted fixed-point vector (RFPV) as follows:

$$FPV_2 = (\rho_{[\theta]_1, C_1}, \rho_{[\theta]_1, C_2}, \rho_{[\theta]_1, C_s}, \dots, \rho_{[\theta]_1, D_{3h}}) = (4, 2, 2, 4, 1, 2, 1, 1, 1, 1). \tag{40}$$

Similarly, RFPVs for the partitions $[\theta]_2$ (Eq. 14) to $[\theta]_8$ (Eq. 20) are calculated by introducing Eqs. 3–5, Eq. 36, and Eq. 37 into Eq. 35. They are collected to form a restricted fixed-point matrix (RFPM) as follows:

$$FPM_2 = \begin{matrix} [\theta]_2 \\ [\theta]_3 \\ [\theta]_4 \\ [\theta]_1 \\ [\theta]_5 \\ [\theta]_6 \\ [\theta]_7 \\ [\theta]_8 \end{matrix} \begin{pmatrix} 1 & 1 & 1 & 1 & 1 & 1 & 1 & 1 & 1 & 1 \\ 9 & 1 & 3 & 3 & 0 & 1 & 0 & 0 & 0 & 0 \\ 18 & 4 & 4 & 6 & 0 & 2 & 0 & 0 & 0 & 0 \\ 4 & 2 & 2 & 4 & 1 & 2 & 1 & 1 & 1 & 1 \\ 30 & 0 & 4 & 6 & 0 & 0 & 0 & 0 & 0 & 0 \\ 120 & 0 & 8 & 0 & 0 & 0 & 0 & 0 & 0 & 0 \\ 108 & 0 & 8 & 12 & 0 & 0 & 0 & 0 & 0 & 0 \\ 216 & 0 & 8 & 0 & 0 & 0 & 0 & 0 & 0 & 0 \end{pmatrix}. \tag{41}$$

In a parallel way to Eq. 21, note again that the FPM₂ for the partition $[\theta]_1$ (Eq. 40) appears at the 4th row of the FPM₂ (Eq. 41). The values appearing at the third column (the C_s -column) of FPM₂ (Eq. 41) are collected from the generating function for C_s (Eq. 38).

According to Theorem 1, the RFPM is multiplied by the inverse mark table $M_{D_{3h}}^{-1}$ (see Eq. 41) so as to give a restricted isomer-counting matrix (RICM):

$$RICM_2 = FPM_2 \times M_{D_{3h}}^{-1} = \begin{matrix} [\theta]_2 \\ [\theta]_3 \\ [\theta]_4 \\ [\theta]_1 \\ [\theta]_5 \\ [\theta]_6 \\ [\theta]_7 \\ [\theta]_8 \end{matrix} \begin{pmatrix} 0 & 0 & 0 & 0 & 0 & 0 & 0 & 0 & 0 & 1 \\ 0 & 0 & 1 & 0 & 0 & 1 & 0 & 0 & 0 & 0 \\ 0 & 1 & 1 & 0 & 0 & 2 & 0 & 0 & 0 & 0 \\ 0 & 0 & 0 & 0 & 0 & 1 & 0 & 0 & 0 & 1 \\ 1 & 0 & 2 & 1 & 0 & 0 & 0 & 0 & 0 & 0 \\ 8 & 0 & 4 & 0 & 0 & 0 & 0 & 0 & 0 & 0 \\ 6 & 0 & 4 & 2 & 0 & 0 & 0 & 0 & 0 & 0 \\ 16 & 0 & 4 & 0 & 0 & 0 & 0 & 0 & 0 & 0 \end{pmatrix}, \tag{42}$$

Note that each pair of enantiomers is counted once just as each achiral derivative is counted once.

3.3.2 Comparison Between Unrestricted and Restricted Enumerations

Let us compare between the results of the unrestricted enumeration (Eq. 22) and those of the restricted one (Eq. 42). As a matter of course, the $[\theta]_2$ -rows, the $[\theta]_5$ -rows, or the $[\theta]_6$ -rows of both the ICMs are equal to each other, because they do not contain edge substitutions. The $[\theta]_3$ -row (Z) is concerned with substitution of one edge, so that there appears no effect of the restriction condition. Thus, one C_s -derivative or one C_{2v} -derivative is generated by selecting a substitution site from either the $D_{3h}/(C_s)$ -orbit or the $D_{3h}/(C_{2v})$ -orbit. Hence, the $[\theta]_2$ -row of Eq. 22 is identical with the counterpart of Eq. 42.

Derivatives of Z^2 ($[\theta]_4$) are depicted in Fig. 4, which compare the restricted edge substitution (Eq. 42) with the corresponding unrestricted one (Eq. 22). Under the restricted condition, the $[\theta]_4$ -rows of Eq. 42 shows that there are one C_2 -derivative (**26/26**), one C_s -derivative (**28**), and two C_{2v} -derivatives (**29** and **29**), which are depicted in the right-hand part of Fig. 4. On the other hand, under the unrestricted condition, the $[\theta]_4$ -rows of Eq. 22 shows the presence of additional derivatives, i.e., one C_1 -derivative (**25/25**) and one additional C_s -derivative (**27**), which are depicted in the left-hand part of Fig. 4. Note that the C_1 -derivative (**25/25**) and the C_s -derivative (**27**) have a vertex (vertex 4) at which two edge substitutions overlap, so that they are discarded under the restricted condition.

The derivatives of Z^3 ($[\theta]_1$) enumerated under the unrestricted condition (the $[\theta]_1$ -rows of Eq. 22) have been already depicted in Fig. 2. In contrast, the $[\theta]_1$ -rows of Eq. 42 indicates the presence of one C_{2v} -derivative (**12**) and one D_{3h} -derivative (**14** (= **2**)), where the other derivatives collected in Fig. 2 are discarded under the restricted condition.

To evaluate the effects of chiral monodentate ligands, let us examine the numbers of C_s -derivatives, each of which appears at the intersection between the C_s -column (the third column) and the $[\theta]_5$ - (corresponding to $2p\bar{p}$), $[\theta]_6$ - ($4Xp\bar{p}$), $[\theta]_7$ - ($4p\bar{p}Z$), or $[\theta]_8$ -row ($4Xp\bar{p}Z$) of the ICM₂ (Eq. 42). These C_s -derivatives are illustrated in Fig. 5, where each pair of p/\bar{p} is represented by a pair of a black solid circle and a gray one, while each achiral ligand (X) is represented by an open circle. Each edge substitution by a bidentate ligand is represented by a boldfaced straight line. The substituents (monodentate and bidentate ligands) in such a C_s -derivative have no common vertices under the restricted condition. Free vertices represent implicit substitutions of appropriate monodentate ligands of the same kind.

The C_s -derivatives of $[\theta]_5$ ($p\bar{p}$), **31** and **32**, are in a diastereomeric relationship, which is regarded as an extended pseudoasymmetric case, because the exchange of p and \bar{p} transforms **31** to **32**, vice versa.

The addition of an achiral monodentate ligand X (open circle) without destroying the C_s -symmetry of **31** and **32** produces the four C_s -derivatives of $[\theta]_6$ ($Xp\bar{p}$), **33–36**. On the other hand, the addition of a bidentate ligand Z (boldfaced straight line) without destroying the C_s -symmetry of **31** and **32** produces the four C_s -derivatives of $[\theta]_7$ ($p\bar{p}Z$), **37–40**.

The addition of a bidentate ligand Z (boldfaced straight line) to the four C_s -derivatives of $[\theta]_6$ ($Xp\bar{p}$), (**33–36**) without destroying the C_s -symmetry produces the four C_s -derivatives of $[\theta]_8$ ($Xp\bar{p}Z$). These C_s -derivatives of $[\theta]_8$ ($Xp\bar{p}Z$), i.e., **41–42**, can be alternatively generated from the four C_s -derivatives of $[\theta]_7$ ($p\bar{p}Z$), **39** and **40**, by adding an achiral ligand X (open circle) without destroying the C_s -symmetry, while the C_s -derivatives of $[\theta]_7$ ($p\bar{p}Z$), **37** and **38**, are incapable of accommodating an achiral ligand X without destroying the C_s -symmetry.

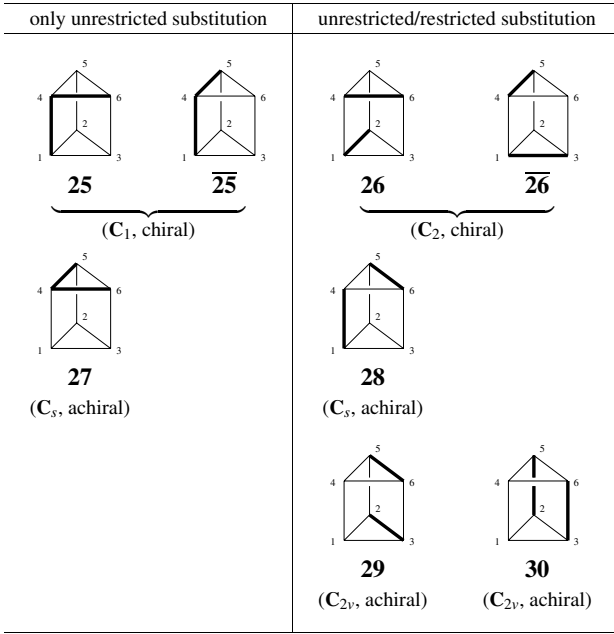


Figure 4: Derivatives of $Z^2([\theta]_4)$. Comparison between unrestricted and restricted edge substitutions.

4 Gross Enumerations under the Restricted Condition

The value B_{θ_i} calculated by Theorem 1 (Eq. 32) is itemized with respect to the subgroup \mathbf{G}_i ($\subset \mathbf{G}$). The total number B_{θ} can be calculated by summing up B_{θ_i} over all \mathbf{G}_i ($i = 1, 2, \dots, s$) as follows:

$$B_{\theta} = \sum_{i=1}^s B_{\theta_i} = \sum_{i=1}^s \sum_{j=1}^s \rho_{\theta_j} \bar{m}_{ji} = \sum_{j=1}^s \rho_{\theta_j} \left(\sum_{i=1}^s \bar{m}_{ji} \right). \tag{43}$$

When the subscript j for the subgroup \mathbf{G}_j runs to cover $j = 1, 2, \dots, s$, the elements $\sum_{i=1}^s \bar{m}_{ji}$ ($j = 1, 2, \dots, s$) construct a column vector, where each element $\sum_{i=1}^s \bar{m}_{ji}$ for j is the sum of the j -th row appearing in the corresponding inverse mark table of \mathbf{G} . Thereby, Eq. 43 is regarded as a multiplication of the row vector (RFPV):

$$(\rho_{\theta_1}, \rho_{\theta_2}, \dots, \rho_{\theta_j}, \dots, \rho_{\theta_s}) \tag{44}$$

by the column vector $(\sum_{i=1}^s \bar{m}_{ji})$.

The number $B_{\theta}^{(a)}$ of achiral derivatives can be calculated by summing up B_{θ_i} over all of the achiral subgroups \mathbf{G}_i selected from \mathbf{G}_i ($i = 1, 2, \dots, s$) as follows:

$$B_{\theta}^{(a)} = \sum_{\forall i_a} B_{\theta_{i_a}} = \sum_{\forall i_a} \sum_{j=1}^s \rho_{\theta_j} \bar{m}_{j i_a} = \sum_{j=1}^s \rho_{\theta_j} \left(\sum_{\forall i_a} \bar{m}_{j i_a} \right). \tag{45}$$

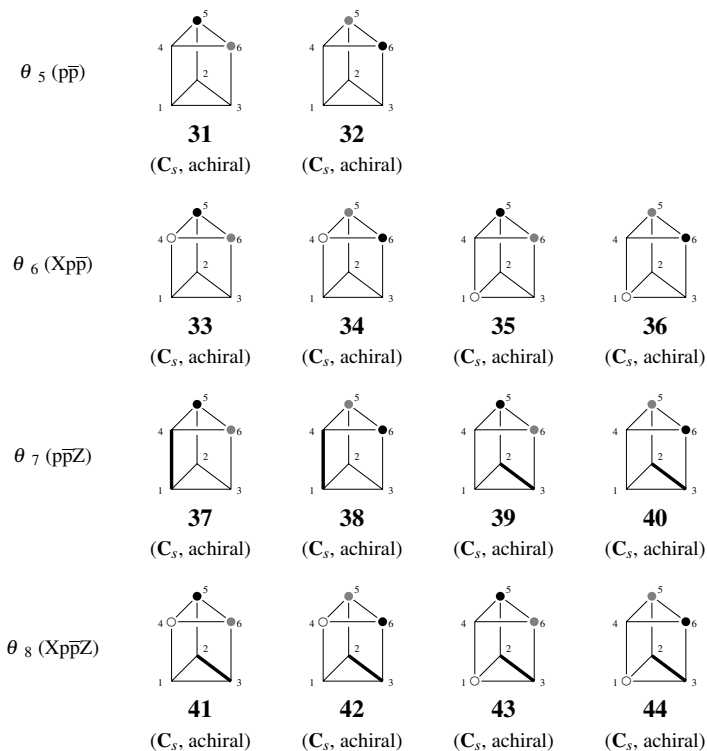


Figure 5: C_s -Derivatives of the formulas, $[\theta]_5$ – $[\theta]_8$, which are characterized by an enantiomeric pair of chiral monodentate ligands, p (black solid circle) and \overline{p} (gray solid circle). Each open circle represents an achiral monodentate ligand and each boldfaced straight line represents a bidentate ligand. These substituents (monodentate and bidentate ligands) in such a C_s -derivative have no common vertices under the restricted condition (Eq. 42).

When the subscript j for the subgroup \mathbf{G}_j runs to cover $j = 1, 2, \dots, s$, the elements $\sum_{\forall i_a} \bar{m}_{ji_a}$ ($j = 1, 2, \dots, s$) construct a column vector, where each element $\sum_{\forall i_a} \bar{m}_{ji_a}$ for j is the sum of the j -th row (only achiral subgroups) appearing in the corresponding inverse mark table of \mathbf{G} .

The number $B_\theta^{(e)}$ of enantiomeric pairs of chiral derivatives can be calculated by summing up $B_{\theta i}$ over all of the chiral subgroups \mathbf{G}_{i_e} selected from \mathbf{G}_i ($i = 1, 2, \dots, s$) as follows:

$$B_\theta^{(e)} = \sum_{\forall i_e} B_{\theta i_e} = \sum_{\forall i_e} \sum_{j=1}^s \rho_{\theta j} \bar{m}_{ji_e} = \sum_{j=1}^s \rho_{\theta j} \left(\sum_{\forall i_e} \bar{m}_{ji_e} \right). \quad (46)$$

When the subscript j for the subgroup \mathbf{G}_j runs to cover $j = 1, 2, \dots, s$, the elements $\sum_{\forall i_e} \bar{m}_{ji_e}$ ($j = 1, 2, \dots, s$) construct a column vector, where each element $\sum_{\forall i_e} \bar{m}_{ji_e}$ for j is the sum of the j -th row (only chiral subgroups) appearing in the corresponding inverse mark table of \mathbf{G} .

To conduct practical calculations, the above-mentioned column vectors generated by Eqs. 43, 45, and 46 are collected to form an $s \times 3$ matrix ($M_{\mathbf{G}}^{(g)}$) for gross enumerations, i.e.,

$$M_{\mathbf{G}}^{(g)} = \begin{array}{c} \mathbf{G}_1 \\ \mathbf{G}_2 \\ \vdots \\ \mathbf{G}_j \\ \vdots \\ \mathbf{G}_s \end{array} \begin{array}{ccc} \text{achiral} & \text{chiral} & \text{total} \\ \left(\begin{array}{ccc} \sum_{\forall i_a} \bar{m}_{1i_a} & \sum_{\forall i_e} \bar{m}_{1i_e} & \sum_{i=1}^s \bar{m}_{1i} \\ \sum_{\forall i_a} \bar{m}_{2i_a} & \sum_{\forall i_e} \bar{m}_{2i_e} & \sum_{i=1}^s \bar{m}_{2i} \\ \dots & \dots & \dots \\ \sum_{\forall i_a} \bar{m}_{ji_a} & \sum_{\forall i_e} \bar{m}_{ji_e} & \sum_{i=1}^s \bar{m}_{ji} \\ \dots & \dots & \dots \\ \sum_{\forall i_a} \bar{m}_{si_a} & \sum_{\forall i_e} \bar{m}_{si_e} & \sum_{i=1}^s \bar{m}_{si} \end{array} \right) \end{array} \quad (47)$$

Thereby, Eqs. 43, 45, and 46 are summarized into a single vector-matrix formulation:

$$\left(B_\theta^{(a)}, B_\theta^{(e)}, B_\theta \right) = (\rho_{\theta 1}, \rho_{\theta 2}, \dots, \rho_{\theta j}, \dots, \rho_{\theta s}) \times M_{\mathbf{G}}^{(g)} \quad (48)$$

This equation corresponds to Eq. 33, where the inverse matrix $M_{\mathbf{G}}^{-1}$ is replaced by the gross-enumeration matrix $M_{\mathbf{G}}^{(g)}$. Note that $M_{\mathbf{G}}^{(g)}$ is derived from $M_{\mathbf{G}}^{-1}$.

The row vector in the left-hand side of Eq. 48 is called a *gross restricted isomer-counting vector* (GRICV) represented by $\text{RICV}^{(g)} (= (B_\theta^{(a)}, B_\theta^{(e)}, B_\theta))$. The row vector in the right-hand side of Eq. 48 is called a *restricted fixed-point vector* (RFPV), which is equal to the counterpart of Eq. 33. Then, Eq. 48 is symbolically represented as $\text{RICV}^{(g)} = \text{RFPV} \times M_{\mathbf{G}}^{(g)}$. When various formulas for $[\theta]$ are considered, the GRICV ($\text{RICV}^{(g)}$) and the RFPV in Eq. 48 can be transformed into a gross restricted isomer-counting matrix (GRICM) represented by the symbol $\text{RICM}^{(g)}$ and a restricted fixed-point matrix (RFPM) respectively, where each GRICV and each RFPV are row vectors of the respective matrices. Then, the resulting matrix calculation is symbolically represented as $\text{RICM}^{(g)} = \text{RFPM} \times M_{\mathbf{G}}^{(g)}$.

It should be noted that Eq. 48 holds true even if the RFPV ($= (\rho_{\theta 1}, \rho_{\theta 2}, \dots, \rho_{\theta j}, \dots, \rho_{\theta s})$) and the $\text{RICV}^{(g)}$ are changed into an unrestricted (usual) FPV and an unrestricted counterpart (i.e., ICV) respectively, because the gross-enumeration matrix $M_{\mathbf{G}}^{(g)}$ (Eq. 47) can be used commonly.

The data of $M_{\mathbf{D}_{3h}}^{-1}$ in Eq. 22 are converted into the corresponding matrix $M_{\mathbf{D}_{3h}}^{(g)}$ for gross enumerations as follows:

$$M_{\mathbf{D}_{3h}}^{(g)} = \begin{matrix} & \text{achiral} & \text{chiral} & \text{total} \\ \mathbf{C}_1 & \left(\begin{array}{ccc} 0 & \frac{1}{12} & \frac{1}{12} \\ 0 & \frac{1}{4} & \frac{1}{4} \\ \frac{1}{2} & -\frac{1}{4} & \frac{1}{4} \\ \frac{1}{6} & -\frac{1}{12} & \frac{1}{12} \\ 0 & \frac{1}{6} & \frac{1}{6} \\ 0 & 0 & 0 \\ 0 & 0 & 0 \\ \frac{1}{3} & -\frac{1}{6} & \frac{1}{6} \\ 0 & 0 & 0 \\ 0 & 0 & 0 \end{array} \right) \end{matrix} \quad (49)$$

Note that the four subgroups, \mathbf{C}_1 , \mathbf{C}_2 , \mathbf{C}_3 , and \mathbf{D}_3 , are chiral, while the six subgroups, \mathbf{C}_s , \mathbf{C}'_s , \mathbf{C}_{2v} , \mathbf{C}_{3v} , \mathbf{C}_{3h} , and \mathbf{D}_{3h} , are achiral.

By using the fixed-point matrix shown in Eq. 41, the gross enumeration corresponding to the itemized enumeration shown in Eq. 42 can be conducted so as to give the following gross restricted isomer-counting matrix ($\text{ICM}_2^{(g)}$):

$$\text{ICM}_2^{(g)} = \text{FPM}_2 \times M_{\mathbf{D}_{3h}}^{(g)} = \begin{matrix} & \text{achiral} & \text{chiral} & \text{total} \\ \begin{matrix} [\theta]_2 \\ [\theta]_3 \\ [\theta]_4 \\ [\theta]_1 \\ [\theta]_5 \\ [\theta]_6 \\ [\theta]_7 \\ [\theta]_8 \end{matrix} & \left(\begin{array}{ccc} 1 & 0 & 1 \\ 2 & 0 & 2 \\ 3 & 1 & 4 \\ 2 & 0 & 2 \\ 3 & 1 & 4 \\ 4 & 8 & 12 \\ 6 & 6 & 12 \\ 4 & 16 & 20 \end{array} \right) \end{matrix} \quad (50)$$

For example, the right part of Fig. 4 verifies the $[\theta]_4$ -row of the ICM shown in Eq. 50. Thus, there are three achiral derivatives (**28**, **29**, and **30**), one enantiomeric pair of **26/26**, and totally four derivatives.

5 Conclusion

The USCI approach is extended to be capable of combinatorial enumerations of 3D structures or graphs under a restricted condition, where orbits of vertices and edges interact each other. Territory indicators of vertices or edges are defined to convert SCI-CFs (for an unrestricted condition) into restricted SCI-CFs, by which the interaction of adjacent edges or the interaction between a vertex and its incident edge is avoided. The extension of the FPM method among the four methods of the USCI approach is mainly discussed in this paper.

References

- [1] S. Fujita, "Symmetry and Combinatorial Enumeration in Chemistry," Springer-Verlag, Berlin-Heidelberg (1991).
- [2] S. Fujita, "Diagrammatical Approach to Molecular Symmetry and Enumeration of Stereoisomers," University of Kragujevac, Faculty of Science, Kragujevac (2007).

- [3] S. Fujita, *Theor. Chim. Acta*, **76**, 247–268 (1989).
- [4] S. Fujita, *J. Math. Chem.*, **5**, 121–156 (1990).
- [5] S. Fujita, *Bull. Chem. Soc. Jpn.*, **63**, 203–215 (1990).
- [6] S. Fujita, *Bull. Chem. Soc. Jpn.*, **63**, 2759–2769 (1990).
- [7] S. Fujita, *Bull. Chem. Soc. Jpn.*, **64**, 3215–3223 (1991).
- [8] S. Fujita, *Bull. Chem. Soc. Jpn.*, **62**, 3771–3778 (1989).
- [9] S. Fujita, *Tetrahedron*, **46**, 365–382 (1990).
- [10] S. Fujita, *Bull. Chem. Soc. Jpn.*, **63**, 1876–1883 (1990).
- [11] S. Fujita, *J. Math. Chem.*, **7**, 111–133 (1991).
- [12] S. Fujita, *J. Chem. Inf. Comput. Sci.*, **36**, 270–285 (1996).
- [13] S. Fujita and N. Matsubara, *Internet Electronic Journal of Molecular Design*, **2**, 224–241 (2003).
- [14] S. Fujita, “Computer-Oriented Representation of Organic Reactions,” Yoshioka-Shoten, Kyoto (2001).
- [15] According to the private communications from V. R. Rosenfeld and D. J. Klein, they have recently developed an alternative method for investigating such restricted cases effectively, where Pólya’s cycle indices [17, 18] are refined [19] and integrated with the inclusion-exclusion procedure [20]. The author is grateful to Prof. Rosenfeld for sending me preprints of their articles. These articles have prompted us to report the present article and related ones as an extended version of the USCI approach for examining restricted cases.
- [16] N. N. Greenwood and A. Earnshaw, “Chemistry of the Elements,” Pergamon Press, Oxford (1984).
- [17] G. Pólya, R. E. Tarjan, and D. R. Woods, “Notes on Introductory Combinatorics,” Birkhäuser, Boston (1983).
- [18] G. Pólya and R. C. Read, “Combinatorial Enumeration of Groups, Graphs, and Chemical Compounds,” Springer-Verlag, New York (1987).
- [19] V. R. Rosenfeld, *MATCH Commun. Math. Comput. Chem.*, **43**, 111–130 (2001).
- [20] A. Kerber, “Applied Finite Group Actions,” Springer Verlag, Berlin, Heidelberg (1999).